Acoustic waveform inversion with application to seasonal snow covers

Donald G. Albert[a)]
US Army Cold Regions Research and Engineering Laboratory, 72 Lyme Road, Hanover, New Hampshire 03755-1290

(Received 10 March 1997; revised 16 August 1997; accepted 2 October 2000)

The amplitude and waveform shape of atmospheric acoustic pulses propagating horizontally over a seasonal snow cover are profoundly changed by the air forced into the snow pores as the pulses move over the surface. This interaction greatly reduces the pulse amplitude and elongates the waveform compared to propagation above other ground surfaces. To investigate variations in snow-cover effects, acoustic pulses were recorded while propagating horizontally over 11 different naturally occurring snow covers during two winters. Two inversion procedures were developed to automatically match the observed waveforms by varying the snow-cover parameters in theoretical calculations. A simple frequency-domain technique to match the dominant frequency of the measured waveform suffered from multiple solutions and poor waveform matching, while a time-domain minimization method gave unique solutions and excellent waveform agreement. Results show that the effective flow resistivity and depth of the snow are the parameters controlling waveform shape, with the pore shape factor ratio of secondary importance. Inversion estimates gave flow resistivities ranging from 11 to 29 kN s m^{-4}, except for two late-season cases where values of 60 and 140 were determined (compared to 345 for the vegetation-covered site in the summer). Acoustically determined snow depths agreed with the measured values in all but one case, when the depth to a snow layer interface instead of the total snow depth was determined. Except for newly fallen snow, the pore shape factor ratio values clustered near two values that appear to correspond to wet (1.0) or dry (0.8) snow. [DOI: 10.1121/1.1328793]

PACS numbers: 43.28.En, 43.28.Fp, 43.60.Pt [LCS]

I. INTRODUCTION

The interaction of sound energy with the ground is an important effect in understanding outdoor sound propagation.[1–3] It affects predictions of traffic, industrial, or blasting noise levels, which are becoming increasingly important in mitigating or preventing community noise problems and assessing environmental impacts of various activities. Snow is of interest in these applications since it is the most absorbent, naturally occurring ground cover. The presence of a snow cover has a large effect on acoustic pulse propagation, causing increased attenuation and marked waveform changes compared with propagation over grassland.[4] This article reports on measurements that were undertaken during two winters to investigate a wide range of snow covers and to examine the effect of snow cover properties on acoustic pulse propagation outdoors. The feasibility of using acoustic measurements to automatically determine properties of the snow itself is also examined.

Although it has long been known that a snow cover strongly absorbs sound, there are still significant experimental data gaps limiting the understanding and ability to predict acoustic wave interaction with snow.[5] Early papers on acoustics and snow were rather infrequent, and primarily reported that snow strongly absorbed audible acoustic waves, either through anecdotal reports,[6,7] simple measurements,[8] or simple calculations.[9] In all of these papers, the effect of various snow properties or structures was ignored. It was not recognized until the 1950's that the physical properties of the snow and snow metamorphism had an effect on the acoustic properties of the snow. Careful experimental measurements were reported by a number of Japanese researchers,[10–18] who conducted short-range acoustic measurements using loudspeakers and continuous wave (CW) sources in and above a snow cover, and reported differences between the propagation characteristics of ''new'' and ''compact'' snow. This work is summarized in Refs. 11 and 19. Short range measurements were also reported by Tillotson.[20] Gubler[21] reported on measurements of peak amplitude decay for propagation experiments on a shallow snow cover using an explosion source.

Johnson[22] was the first to apply Biot's[23–25] complete and comprehensive treatment of wave propagation in a porous medium to snow. However, for acoustic waves propagating above a snow cover, the full Biot theory is not necessary, since treating the snow as a rigid-framed porous material is sufficient to describe the air flow within the pores, and the elastic properties of the ice grain bonds have little effect. This simplified theory has been widely used to treat ground effects in outdoor sound propagation over soils and grass.[26] Various formulations have been developed to model the acoustic effects of the rigid porous material; Delaney and Bazley[27] developed an empirical relation that is widely used; Attenborough's[28] four-parameter model (the parameters are effective flow resistivity, porosity, and two shape factors) is theoretically based. These rigid-frame models have been

a)Electronic mail: dalbert@crrel.usace.army.mil

used to analyze data from short-range, high-frequency CW measurements over snow,[29,30] pulse measurements at longer ranges and lower frequencies,[31] and laboratory measurements on snow samples;[32,33] the physically based model has been shown to give better agreement than the Delaney–Bazley empirical model.

In this paper, experimental measurements of acoustic pulse propagation over seasonal snow covers are reported. The measurements were conducted over two winters to investigate the variations in acoustic response caused by naturally occurring variations in the snow-cover parameters. The next section of this paper discusses the experimental approach. A waveform inversion method is developed to determine the snow-cover parameters from the acoustic measurements and applied in the following section, and the acoustically determined parameters of the snow are compared to the directly observed snow properties. These results are discussed and summarized in the final section.

II. EXPERIMENTAL MEASUREMENTS

The experimental objective was to determine the acoustic response and its variability for typical New England seasonal snow covers. To accomplish this goal, broadband acoustic pulses were recorded as they propagated horizontally above the soil or snow surface at an undisturbed site in Hanover, NH. As the snow-cover properties changed during two winters, the measurements were repeated at the same location with an identical experimental setup. Careful characterization measurements were also done to allow the acoustic results to be compared to the snow-cover properties and other environmental conditions. Snow-cover characteristics change, and not only as a result of deposition from storms or melting during thaw periods. Snow continually metamorphoses as a result of temperature and vapor gradients within it,[34] and one of the goals of these experiments was to investigate how such physical changes within the snowpack affect the acoustic response.

A handheld .45-caliber blank pistol fired 1 m above the soil or snow surface was used as the source of the acoustic waves. The acoustic pulses were monitored using a linear array of 4.5-Hz Mark Products model L-15B geophones and Globe model 100C low-frequency microphones located at the soil or snow surface at distances up to 90 m away from the source. In addition, two Bruel & Kjaer type 4165 microphones were used to record the source pulse. A Bison model 9048 digital seismograph, triggered by a microphone located near the pistol, was used to record the waveforms at a sampling rate of 5 kHz per channel. The useful bandwidth of the measurements is estimated as 5–500 Hz and is limited mainly by the source output and the high frequency roll-off of the Globe microphones (see Fig. 1).

For each winter experiment, a snow characterization pit was used to determine the temperature, density, wetness, grain size, and crystal type for each layer present, using standard techniques.[35] Snow and frost depths were also measured throughout the test site. The ground was always frozen to at least 0.10 m depth during the winter measurements.

Meteorological data were collected using a Campbell Scientific model 21X data logger. Temperatures were measured within the ground and snow and at heights of up to 5 m in the air. Wind speeds at 1- and 3-m heights were also recorded, along with relative humidity and barometric pressure. All of the experiments were conducted on days of light or no wind and over short propagation ranges, so the atmospheric conditions introduced little variability in the acoustic measurements.

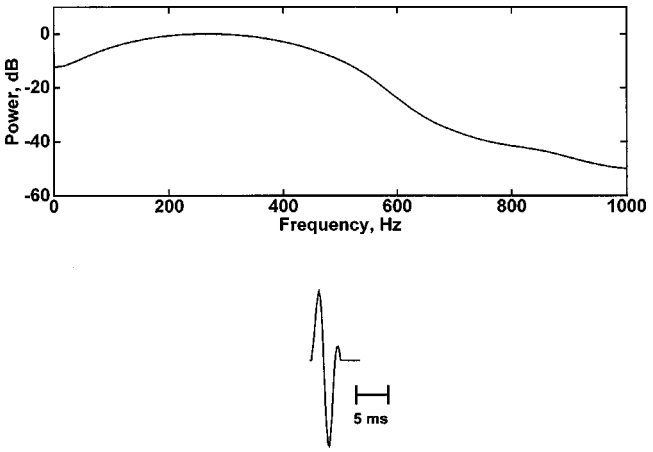

FIG. 1. Estimated source pulse from the blank pistol (bottom) and calculated power spectral magnitude (top). Because measurements of the source pulse made using a microphone 10 m away were influenced by ground reflections (and were often clipped), this source pulse is *estimated* by smoothing a measured waveform. The source spectrum shows the frequency bandwidth of the measurements.

Seismic refraction measurements taken under summer conditions indicated a compressional wave velocity of 265 $m\,s^{-1}$ at the surface, with the velocity rapidly increasing to about 400 $m\,s^{-1}$ within the upper meter. Laboratory analysis of soil samples showed that the soil type throughout the test area was a silty sand. The soil moisture content during the summer experiment was 25%.

Figure 2 summarizes the experimental measurements obtained. The figure shows the normalized pressure waveform recorded by a surface microphone 60 m away from the source location, for 11 different snow covers and for grass-covered ground. The waveforms recorded over snow are all elongated to various degrees, and exhibit relatively stronger low-frequency content than those recorded without snow present. This change in waveform shape when snow is present is mainly attributable to the existence of an acoustic surface wave above the highly absorbing snow surface.[36] The differences in the recorded waveforms are caused by changes in the snow-cover properties, which are also shown schematically in Fig. 2 and listed in Table I. These waveform changes will be examined more closely below when the inversion method is developed.

Two of the tests, experiments 11 and 12, occurred during the spring melt period. For these tests, the entire snowpack had ''ripened''; it had been at the melting point for some time, allowing the ice grains to become very large, and was rapidly melting. The snow cover was becoming very nonuniform in depth and discontinuous in some areas as the melt season progressed. These measurements showed the smallest waveform elongations recorded during the winter.

For each of the experiments, the peak pressure of the

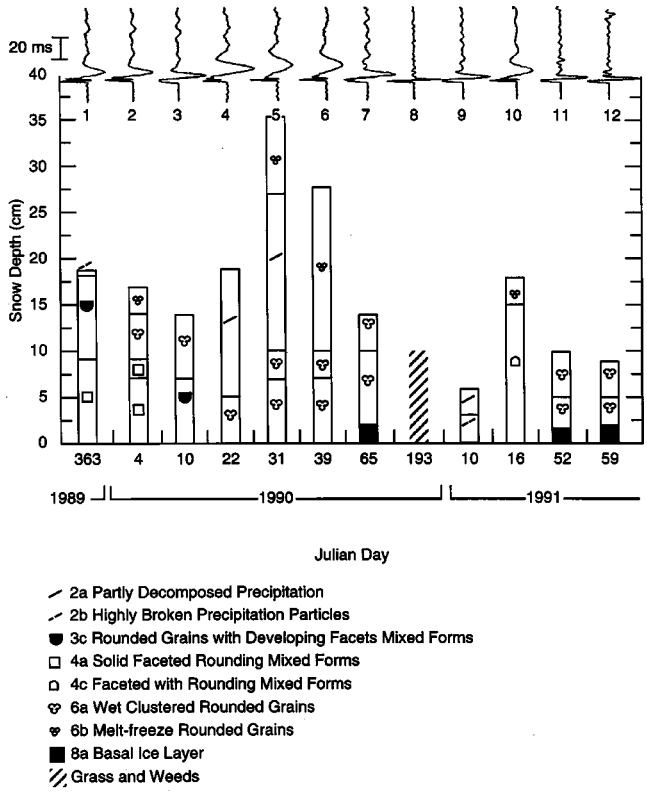

FIG. 2. Chronological evolution of snow-cover properties and the acoustic pulses measured after propagating from a source 60 m away. The snow-cover stratigraphy and crystal type are shown below the acoustic waveforms; additional snow-cover properties are listed in Table I. The microphone pressure waveforms are normalized. Experiment numbers indicated on the figure are in chronological order and are used in Tables I–III.

pulses, the amplitude decay with distance, and the acoustic-to-seismic coupling ratio, defined as the ratio of induced particle velocity in the snow to the incident acoustic pressure, were determined from the data and are listed in Table II. With the exception of the two measurements made during the melt period, the peak pressure at 60 m range was smaller by a factor of 3–7 than the peak pressure measured in the summer. This reduction in peak pressure is caused by increased transmission of sound energy into the subsurface as the pulses interact with the highly permeable snow cover in the winter.

The amplitude decay as a function of range was determined by least-squares fitting of the data from the surface microphones at all ranges to the expression

$$A(r)=A_1 r^{\alpha}, \tag{1}$$

where r is the propagation distance in m, $A(r)$ is the peak amplitude in Pa at range r, A_1 is the source amplitude at a reference distance r_1, and α is the distance attenuation exponent. The coefficient α for snow (Table II) is about -1.8 over snow (slightly lower during the melt period) compared to a value of -1.4 for the grass- and weed-covered ground in the summer. These values agree with previous longer-range pulse measurement values of -1.9 for snow and -1.2 for grass-covered soil.[4]

The acoustic-to-seismic coupling was determined from the collocated surface vertical component geophones and surface microphones (Table II). These ratios vary from 2 to $16\times10^{-6}\,\mathrm{m\,s^{-1}\,Pa^{-1}}$ and are in agreement with previous measurements.[4,37–40]

III. ACOUSTIC WAVEFORM ANALYSIS

The experimental data collected show that the acoustic pulse shapes are greatly affected by the presence of a snow cover. In this section, a method for automatically modeling these waveform changes and using this model to determine the physical characteristics of the snow cover is developed.

A. The forward problem: Calculating pulse shapes from known surface properties

Although most previous work in outdoor sound propagation used continuous wave sources, a few studies have used pulses, which are a much more stringent test of related acoustic theories. A method of calculating pulse shapes based on the Delaney–Bazley empirical model[27] of ground impedance has been developed[41–44] and applied to investigations of soil properties.[41,42,45,46] This work has been extended[31] by including a more complicated but physically based model of ground impedance.[28] The new model gave better agreement with observed measurements for snow, primarily because of its increased accuracy at low frequencies compared to the empirical model.

The procedure for calculating theoretical acoustic pulse waveforms from known (or assumed) surface properties is briefly outlined here. For a monofrequency source in the air and a receiver on the surface, the acoustic pressure P a slant distance r away from the source is given by

$$\frac{P}{P_0}=\frac{e^{ikr}}{kr}(1+Q)e^{-i\omega t}, \tag{2}$$

where P_0 is a reference source level, k is the wave number in air, and Q is the spherical wave reflection factor representing the effect of the ground. At high frequencies ($kr\gg1$), Q can be written as[47–49]

$$Q=R_P+(1-R_P)F(w), \tag{3}$$

where R_P is the plane wave reflection coefficient, F is the boundary loss factor, and w is a numerical distance, all of which depend on the specific surface impedance Z of the ground. The impedance is itself dependent upon frequency; thus, so is Q. [The elongation and relatively stronger low frequency content of the measured waveforms in Fig. 2 can be explained theoretically by the decrease in R_P at high frequencies and the enhancement of $F(w)$ at low frequencies (see Ref. 31, Fig 4).] For a particular frequency f_n (denoted by subscript n), once Q_n is determined, the response P_n can be written as

$$P_n=\frac{P_0}{4\pi r}S_n W_n(1+Q_n)e^{i2\pi f_n r/c}, \quad n=0,1,2,\ldots,N-1 \tag{4}$$

where S_n and W_n represent the source and instrument effects, respectively, and c is the speed of sound in air. An inverse FFT

TABLE I. Snow cover properties.

Experiment number	Date/ Julian day	Air temperature, °C	Height above base, cm	Snow temperature, °C	Grain classification[a]	Grain size, mm	Density, kg m^{-3}	Wet snow? (Dye test)
1	12-29-89	−13.5	0–9	−5.0	4a	4	170	N
	363		9–18	−9.5	3c	2	150	N
			18–18.5	−13.5	2b	1.5		N
2	1-4-90	4.0	0–7	0	4a	3	220	⋯
	4		7–9	0	4a	3	220	⋯
			9–14	0	6b	2	200	⋯
			14–17	0	6a	1	260	Y
3	1-10-90	1.5	0–7	−1.0	3c	3	240	N
	10		7–14	0	6b	2	280	Y
4	1-22-90	−5.0	0–5	−2.5	6b	0.5	210	N
	22		5–12	−3.0	2a	0.5	130	N
			12–19	−3.0	2a		100	N
5	1-31-90	−3.0	0–7	0	6b	1.0	260	N
	31		7–10	−0.5	6b	0.8	240	N
			10–27	−2.5	2a	0.25	120	N
			27–35.5	0	6a	0.25	140	N
6	2-8-90	5.0	0–7	0	6b	2	180	N
	39		7–10	0	6b	2	220	Y[b]
			10–19	0	6a	2	200	Y[b]
			19–28	0	6a		150	Y[b]
7	3-6-90	−2.0	0–2	−1.0	8c	⋯	>400	N
	65		2–10	−1.0	6b	1	290	N
			10–14	0	6b	1	340	N
8	7-12-90	18.0	0–10	Grass and weed covered soil				
	193							
9	1-10-91	−10.5	0–3	−5.0	2b	1	100	N
	10		3–6	−6.0	2a	4	100	N
10	1-16-91	2.0	0–5	−0.5	4c	0.5	190	N
	16		5–10	−0.5	4c	0.5	150	N
			10–15	−0.5	4c	0.75	140	N
			15–18	−0.5	6a	1	210	Y
11	2-21-91	6.0	0–1.5	0	8c	⋯	>400	Y
	52		1.5–5	0	6b	12	310	Y
			5–10	0	6b	8	270	Y
12	2-28-91	1.0	0–2	0	8c	⋯	>400	Y
	59		2–5	0	6b	4	220	Y
			5–9	0	6b	7	250	Y

[a]Snow grain types are given in accordance with the international standard; see Ref. 35. See Fig. 1 caption for grain types.
[b]During the acoustic experiments, which were conducted in the morning, the snow cover was cold and no liquid water was present. The snow warmed up considerably by the time the snow pit was done at noon.

$$P_m = \frac{1}{N}\sum_{n=0}^{N-1} P_n e^{-i2\pi mn/N}, \quad m = 0,1,2,...,N-1 \tag{5}$$

is used to construct theoretical pulse waveforms in the time domain. Nicolas *et al.*[29] have shown that an explicitly layered model of the ground must be used to represent thin snow covers, and this was done in the calculations presented here using (omitting the frequency subscripts)

$$Z = Z_2 \frac{Z_3 - iZ_2 \tan k_2 d}{Z_2 - iZ_3 \tan k_2 d}, \tag{6}$$

where d is the snow layer thickness, k_2 is the wave number in the layer, and Z_2 and Z_3 are the impedances of the snow layer and substratum, respectively (Ref. 50, p.17).

The acoustic behavior of the soil or snow is specified by the specific impedance Z_2 and wave number k_2, which are used in Eqs. (3) and (6) to find the theoretical waveform. A number of models are available in the literature to calculate these parameters.[51] In this paper, the parameters were calculated using Attenborough's[28] four-parameter model of ground impedance. The four input parameters are the effective flow resistivity σ, the porosity Ω, the pore shape factor ratio s_f, and the grain shape factor n'. The snow depth d and the substrate properties are also required in a layered model.

Attenborough's model describes propagation in the porous medium via the propagation constant k_2 and the characteristic impedance Z_c (which is the same as the surface impedance for a locally reacting material)

$$k_2 = \frac{\omega}{c_0} q \frac{C^{1/2}}{B^{1/2}}, \tag{7}$$

$$\frac{Z_c}{\rho_0 c_0} = \frac{q}{\Omega} \frac{1}{B^{1/2} C^{1/2}}, \tag{8}$$

where

TABLE II. Range decay coefficient and acoustic-to-seismic coupling ratio measured for air waves. The error bounds are 95% confidence intervals.

Experiment number	Date	Range decay coefficient α		Acoustic-to-seismic coupling ratio, $m\,s^{-1}\,Pa^{-1}$		Peak amplitude at 60 m Pa
		Number of points	α	Number of points	Ratio $\times 10^{-6}$	
1	363-89	32	-1.9 ± 0.4	31	1.9 ± 0.2	3.7
2	04-90	13	-1.8 ± 0.4	60	3.1 ± 0.3	5.3
3	10-90	18	-1.7 ± 0.2	80	2.9 ± 0.2	5.0
4	22-90	42	-1.6 ± 0.3	42	5.6 ± 0.7	2.1
5	31-90	40	-1.8 ± 0.4	40	16.2 ± 1.5	2.3
6	39-90	35	-1.7 ± 0.3	35	7.3 ± 0.5	2.0
7	65-90	18	-1.8 ± 0.3	36	3.1 ± 0.3	3.3
9	10-91	68	-1.9 ± 0.2	59	2.9 ± 0.3	4.0
10	16-91	50	-1.8 ± 0.2	50	10.8 ± 0.8	2.9
11	52-91	91	-1.6 ± 0.1	89	3.6 ± 0.2	6.6
12	59-91	76	-1.4 ± 0.1	76	4.7 ± 0.3	7.3
8	193-90	48	-1.4 ± 0.2	27	4.1 ± 0.9	13.8

$$B=\left[1-\frac{2}{D}T(D)\right],\quad C=\left[1-\frac{2(\gamma-1)}{N_{\mathrm{Pr}}^{1/2}D}T(N_{\mathrm{Pr}}^{1/2}D)\right],$$

$T(x)=[J_1(x)]/[J_0(x)]$
is the ratio of cylindrical Bessel functions,

$$\lambda=\frac{1}{s_f}[(8\rho_0 q^2\omega)/(\Omega\sigma)]^{1/2},\quad D=\lambda\sqrt{i},$$

$q^2=\Omega^{-n'}=$tortuosity,

γ=the ratio of specific heats (=1.4 for air), N_{Pr}=Prandtl number (=0.71 for air), and $\omega=2\pi f$.

For all of the calculations in this paper, the grain shape factor n' was set to 0.5 corresponding to spherical grains, and the porosity Ω was determined from the measured density of the snow. Parameters for the frozen soil beneath the snow were fixed at $\sigma=3000$ kN s m^{-4}, $\Omega=0.27$, $s_f=0.73$, and $n'=0.5$.[31] The effective flow resistivity σ, the snow depth d, and the pore shape factor ratio s_f were varied in the inversions discussed below.

B. The inverse problem: Finding snow parameters to match the observed acoustic waveforms

The previous section discussed the *forward* problem, using a rigid-ice-frame porous model of snow to calculate the expected waveform shape when the snow properties are measured or assumed. Through trial-and-error calculations, good agreement between the calculated and observed waveforms can often be obtained.[31] However, this procedure is time consuming and tedious, and does not provide information about the uniqueness of the waveform match or the sensitivity of the calculated waveforms to the snow parameters. In this section, the *inverse* problem is investigated, where the observed waveform is used to determine automatically the acoustic parameters of the snow. Two inversion strategies, one in the frequency domain and one in the time domain, were investigated in an attempt to match the experimentally observed waveforms.

1. Frequency-domain inversion

The elongated, low-frequency acoustic surface wave is a dominant characteristic of the pulse waveforms observed propagating over a snow cover (see Fig. 2). The first inversion attempt, therefore, was to try to match the dominant frequency of the observed waveform, since this frequency should sensitively depend on the snow-cover properties responsible for the acoustic surface wave shape. If successful, this inversion procedure would be extremely rapid, since the broadband time-domain waveform would not need to be calculated as part of the search procedure. Fast methods of finding the peak frequency from a given set of assumed acoustic parameters could be developed to further reduce the calculation times.

Unfortunately, problems were encountered when this inversion strategy was tested. Figure 3 shows a simplified example of the inversion. In this figure, the snow depth was held at the measured value of 0.28 m at the sensor location, and the pore shape factor ratio s_f is fixed at a value of 0.8. Only the effective flow resistivity σ was allowed to vary in calculating the theoretical peak frequency. The figure shows that there are two solutions; that is, there are two values of the flow resistivity that give agreement with the observed peak frequency. This *nonuniqueness* of solutions is a common feature of inversions, and indicates that the information content of the measurements is not enough to require a single parameter value to obtain agreement. There are a number of approaches one can take to investigate this nonuniqueness.[52]

However, these approaches were not considered because the problem is more serious than just finding multiple solutions. Figure 4 shows a comparison of the observed and theoretical waveforms; the agreement is very poor. Apparently, the frequency-domain representation of the observed waveform has a very broad spectral maximum. Thus, matching this parameter is not sufficiently sensitive to yield good waveform agreement as had been hoped. Although the method had the promise of very rapid calculations and inversions, it had to be abandoned because of its poor accuracy.

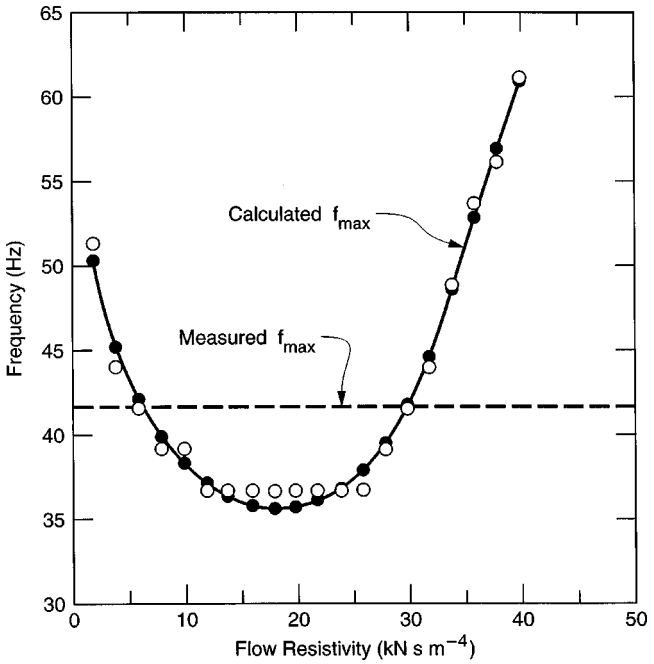

FIG. 3. A simplified example of the frequency-domain inversion for the acoustic waveform for experiment 6. The dashed line indicates the peak frequency found by Fourier analysis of the measured waveform, about 42 Hz. The symbols indicate theoretical peak frequencies, open circles represent the FFT bin, and filled circles (connected by the solid line) the interpolated frequency value. The x axis is the flow resistivity σ used to calculate the theoretical peak frequency. The snow depth is held at the measured value of 0.28 m at the sensor, and pore shape factor ratio s_f is fixed at a value of 0.8. Only the effective flow resistivity σ is allowed to vary.

2. Time-domain waveform inversion

In this section, an inversion procedure for directly matching the normalized, time-aligned microphone waveform is discussed. Theoretical waveforms are calculated using Attenborough's[28] model of ground impedance and Eqs. (2)–(6) as discussed above. For the snow, a single snow layer is used, with the effective flow resistivity σ, the snow depth d, and the pore shape factor ratio s_f being allowed to vary; parameters for the frozen soil below the snow are fixed at $\sigma=3000$ kN s m^{-4}, $\Omega=0.27$, $s_f=0.73$, and $n'=0.5$. For the summer case, a half-space model of the ground with the same variable parameters is used.

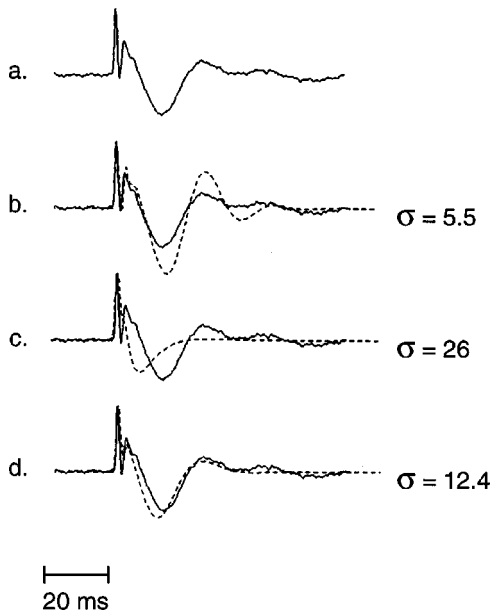

FIG. 4. Comparison of the observed (solid lines) and calculated (dashed lines) waveforms. (a) Measured pulse. (b), (c) Using the frequency domain inversion procedure and the parameters determined from Fig. 3. The agreement is very poor. (d) Using the time-domain inversion procedure shows much better agreement.

In setting up an inverse problem, one has a choice of a norm (or measure) of what is considered to be a good solution. Solutions are then compared using that norm, with the best solution having the minimum value. In this case, the norm was chosen to directly match the theoretical and observed waveforms. The best-fitting waveform was selected under the L_1 norm criterion (i.e., the sum of the absolute value of the differences between the calculated and observed waveforms over a fixed time window) by minimizing

$$\text{Error}=\sum_{t=0}^{\text{waveform}} |P_t^{\text{obs}}-P_t^{\text{calc}}|. \tag{9}$$

A least-squares criterion, the L_2 norm, was avoided because it heavily weights, and tries to reduce, the maximum misfit. Since the source pulse in the calculations is an estimated one, and not actually measured for each experiment, this approach allows for errors in this estimated source pulse to be ignored while accurately fitting the overall, low-frequency portion of the measured waveforms. However, as will be shown below, the waveform agreement turned out to be so close that the choice of norm had no effect on the results, and tests done using the L_2 norm gave the same results.

Before discussing the actual results of this inversion method, a simpler two-parameter inversion example is examined as an illustration. In the actual inversions, the pore shape factor ratio parameter had a small effect on the waveform fits, so it was held constant for this example. Changes in the effective flow resistivity and snow depth had a much larger effect on the theoretical waveform shape. Figure 5 shows these effects by comparing the observed waveform with calculated waveforms for a subset of values of the flow resistivity and snow depth parameters. The best parameters, $\sigma=12.5$ kN s m^{-4} and $d=0.19$ m, are easy to determine by eye and give excellent waveform agreement.

Figure 6 shows the error surface calculated for this experiment as the snow depth and effective flow resistivity were varied in the theoretical calculations. Even over this very large range of parameters, the surface is smooth and has only a single minimum. The appearance of this surface is very encouraging and unusual for an inverse problem, since the single minimum shows that there is only one best solution, and the smoothness of the surface indicates that it will be easy to find that solution, as apparently no local minima exist that could confuse a search procedure.

To find the best waveform fit, a simplex iterative search procedure[53] was implemented, with three variables: the effective flow resistivity σ, the snow depth d, and the pore shape factor ratio s_f. The waveform comparison was calculated for three initial triplets (with unrealistic starting parameter values), and these values were then used to estimate the gradient of the surface and select the next points to be tested.

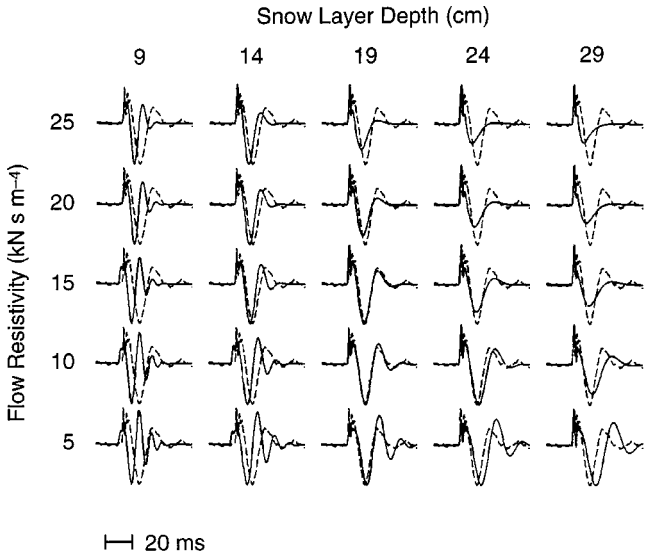

FIG. 5. Visual comparison of the agreement between the observed (dashed lines) and theoretical (solid lines) waveforms for experiment 4. The best fit occurs when the snow depth is 0.19 m and the effective flow resistivity is about 12.5 kN s m^{-4}, in agreement with the surface minimum shown in Fig. 6.

The algorithm moved smoothly and directly to the solution in all cases; restarts with different initial values led to the same final solution. The results of the inversions presented below indicate that the smooth shape of the error surface with a single minimum, as shown in Fig. 6, appears to be a general property, as all of the data waveforms were inverted without encountering any uniqueness or convergence problems. Because of the smoothness of the error surface, a less-conservative convergence procedure would probably work well and increase the search speed. Figure 4 shows the improvement in waveform matching obtained using the time-domain search procedure instead of the frequency-domain inversion.

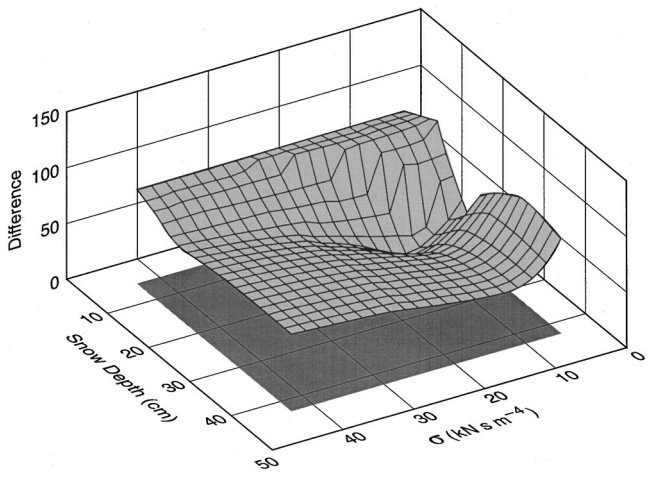

FIG. 6. Comparison of the agreement between observed and theoretical waveforms for experiment 4, using the norm given by Eq. (9). The snow depth and effective flow resistivity are varied in calculating the theoretical waveforms. The best waveform agreement occurs at the minimum of this smooth surface, and the goal of the inversion procedure is to find that minimum.

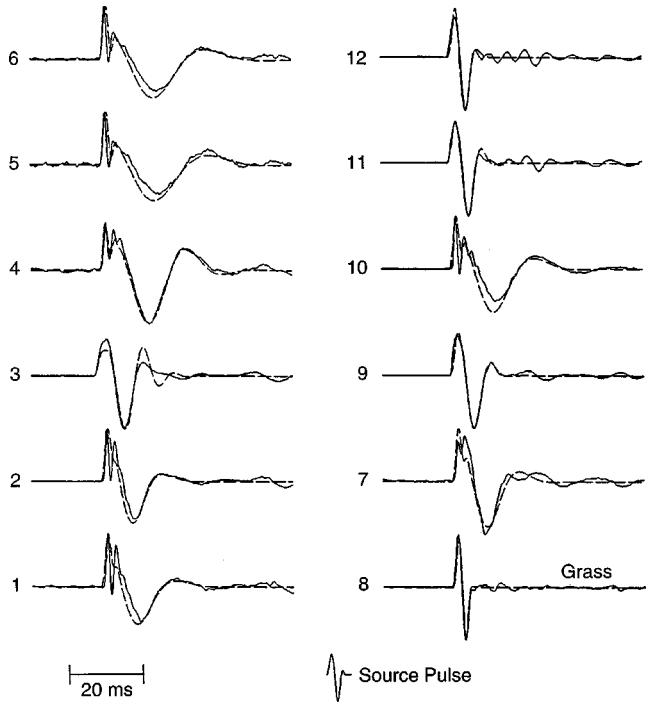

FIG. 7. Comparison of observed (solid lines) and acoustically determined theoretical waveforms (dashed lines) at a propagation distance of 60 m for all of the experiments. The agreement is excellent in all cases. Table II lists the snow parameters found using the waveform inversion procedure.

IV. RESULTS

Figure 7 shows the measured and the theoretical waveforms for all of the experiments. The inversion procedure has been able to automatically match waveforms of quite different appearance, and the agreement is excellent in all cases. Table III gives the snow parameters determined from the acoustic waveform inversion, listed in order of increasing pore shape factor ratio.

The acoustically determined snow depths agree well with the directly measured values. In most cases the agreement is within 0.02 m, which is less than the 0.05-m or greater variation in snow layer thickness along the actual propagation path caused by wind crusts and slight topographic variations. The worst error is 0.05 m, for the thickest snow cover (experiment 5, 0.35 m). In all but one case, the full snow depth was determined. This is not a surprising result considering the large acoustic wavelengths compared to the snow layer thickness. In the exception, experiment 3, the depth to a snow layer interface was determined. An ice layer was not noted at that depth in the snow pit, as might be expected, but a transition occurred from a fine-grained layer above to a coarse-grained layer beneath. This situation has been termed a ''capillary barrier'' to melt water flow through a soil or snow cover.[54,55] Since the daytime high air temperatures had risen to above 0 °C for a few days before this experiment, some melting may have occurred. The melt water would not have penetrated this interface because of the difference in capillary forces, and a very thin ice crust may have formed at this depth, which was overlooked in the snow pit but affected the acoustic wave penetration.

Figure 8 shows the relationship between the half-period

TABLE III. Snow parameters from waveform inversion.

Experiment number	Effective flow resistivity σ, kN s m^{-4}	Acoustic snow depth, cm	Measured snow depth, cm	Pore shape factor ratio, s_f	Wet snow?
6	12	30	28	0.75	Y[a]
7	24	17	14	0.79	N
4	12	19	19	0.80	N
5	11	30	35	0.81	N
1	27	16	18	0.84	N
2	26	14	17	0.93	Y
3	14	9[b]	14	0.97	Y
12	137	3	1–9	0.98	Y
10	11	21	20	0.99	Y
11	58	5	4–10	1.02	Y
9[c]	29	5	6	1.39	N
8[d]	345	⋯	⋯	1.00	N

[a]The snow was wet when the snow pit observations were made, but dry when the acoustic measurements were done earlier that morning.
[b]Depth to a snow layer interface.
[c]Newly fallen snow.
[d]Grass and weed covered ground; no snow present.

of the pressure waveform, defined as the time interval between the peak positive and negative pressures, and the snow depth. This plot shows a strong relationship between the waveform elongation and the snow depth.

The effective flow resistivity values in Table III range from 11 to 29 kN s m^{-4}, except for two late-season cases of discontinuous and very variable snow covers, where values of 58 and 137 were determined. For the grass-covered site in the summer, a value of 345 kN s m^{-4} was determined. These values agree with previous outdoor measurements on snow and soil.[1,3,29–31,56–58] The values also agree with Attenborough and Buser's directly measured values[32,33] of 5 to 17 kN s m^{-4} for alpine snow.

The results listed in Table III for the pore shape factor ratio s_f are of interest, since the values seemed to cluster into two groups, one near 1.0 and the other near 0.8. The value for the only measurement over newly fallen snow was vastly different at 1.4. This parameter is defined as

$$s_f^2 = \frac{8\eta q^2}{\Omega \sigma r_n^2}, \tag{10}$$

where η is the dynamic viscosity of air, q^2 is the tortuosity, Ω is the porosity, σ is the effective flow resistivity, and r_h is the hydraulic radius, defined as twice the area divided by the circumference of the pore cross-sectional shape.

The pore shape factor ratio was clearly secondary in importance, compared to the effective flow resistivity and snow depth, in determining the waveform fits. These two parameters caused very large changes in the waveform shape as they were varied, as can be seen from Fig. 5. The pore shape factor ratio did seem to influence the waveform shapes independently of the other parameters, causing the relative amplitudes of the peaks and troughs to vary, while leaving the overall shape and elongation unchanged. The clustering of the determined values indicates that this parameter may contain information about the pore structure and not just be a free parameter varied randomly to improve the waveform fits.

In all but one experiment, the presence or absence of liquid water in the snow corresponded with the two values of 1.0 and 0.8 (Table III). For the single exception, experiment 6, a closer examination of the field notes and meteorological data (including snow temperature) showed that the snow was wet when the snow pit observations were made, but still cold and dry when the acoustic measurements were done earlier that morning. The presence of liquid water within the snow pack, which tends to gather in the smallest pore necks because of surface tension, could be a physical change responsible for the observed changes in this parameter. The snow pores have complicated shapes and a wide distribution of sizes. Filling the smallest pores with liquid water would remove them from the acoustic interactions, which occur only

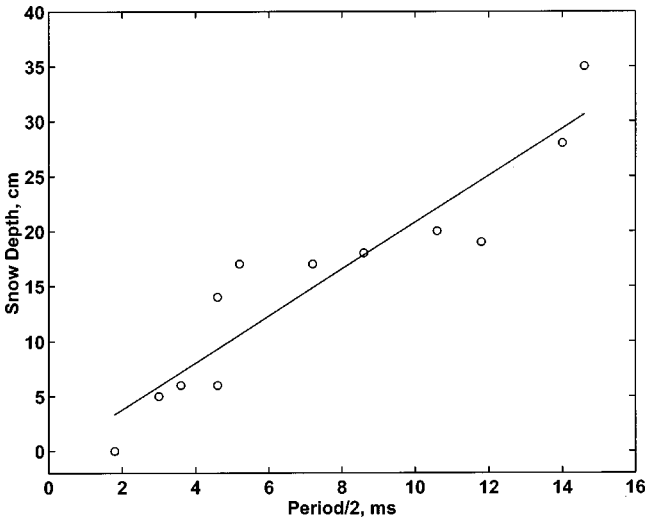

FIG. 8. Half-period of the acoustic waveform vs measured snow depth.

in air-filled pores, perhaps causing the measured change in the pore shape factor ratio parameter. For the newly fallen snow (experiment 9), the pore structure is expected to be quite different because of the much-flatter grain shapes.

Although originally derived as an index of cross-sectional shape, for uniform pores, later work[51,59,60] has shown that the pore shape factor ratio s_f should approach a value of 1 at low frequencies. In addition, comparison with measured data has shown that s_f varies with frequency. Models of acoustic wave propagation in porous materials that explicitly include the effect of pore-size distribution[61–63] have shown that the range of pore sizes present in a material can have measurable effects on the propagation. For these measurements on snow, the determined values of the pore shape factor ratio may be indirectly indicating differences, not in the pore shapes, but in the pore-size distribution. Confirming this hypothesis is left for future work.

Figure 8 shows that the wave elongation is proportional to the snow depth. Are there any other connections between waveform appearance and snow-cover properties? The waveforms for the measurements where the surface layer of the snow was grain type 6a (experiments 2, 5, 6, and 10) are all similar, with a sharp initial pulse followed by a low-frequency surface wave. Also, when the snow surface layer was grain type 6b (experiments 3, 7, 11, and 12), the initial part of the pulse was much more rounded. However, measurements over surface snow of type 2 grains (experiments 1, 4, and 9) have both types of waveforms. Snow-cover depth does consistently divide this set of waveforms into the sharp initial front (experiments 1, 2, 4, 5, 6, and 10) and rounded initial front (3, 7, 9, 11, and 12) classes, depending on whether the snow depth was greater or less than 0.15 m, respectively.

However, the reader is cautioned that these observations are extremely tentative, and must be confirmed by additional observations. In the author's opinion, a much more likely explaination is that atmospheric conditions may control the initial appearance of the waveforms. A slight headwind or upward-refracting temperature gradient would tend to bend the direct ray upwards, reducing its amplitude relative to the surface wave propagating along the surface, while a downwind or downward-refracting condition would tend to enhance this wave.

A subsequent measurement in Alaska[64] showed a dramatic example of this atmospheric effect. Figure 9 shows five waveforms recorded at a range of 202 m over a 3-min interval. The sun had set shortly before the measurements were made, and a strong temperature inversion was rapidly forming. The cooling caused a large amplitude refracted arrival to appear during the course of the measurements, ''sharpening'' the initial part of the waveform, while the surface wave pulse remained unchanged. The snow-cover properties did not change during the short time period of these measurements and cannot have been responsible for the observed waveform changes.

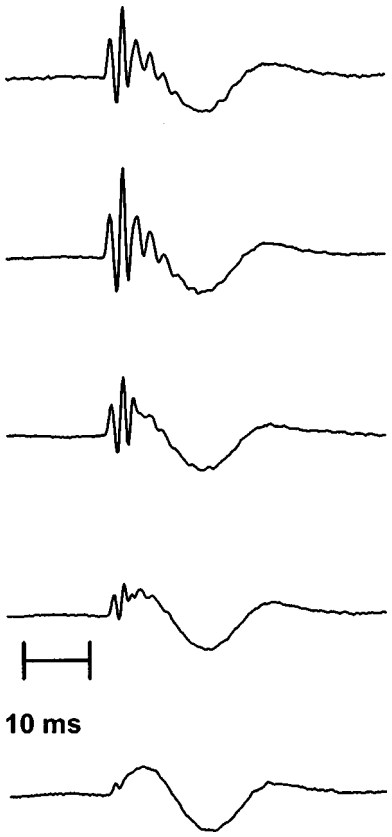

FIG. 9. Blank pistol shot waveforms recorded at a distance of 202 m. These measurements were done over a 3-min period (from bottom to top) in Alaska during the development of an atmospheric inversion layer shortly after sunset. An arrival that is refracted through the air above the snow cover appears and becomes stronger with time as the air cools. (Modified from Ref. 64.)

V. CONCLUDING REMARKS

In this paper, the results of 11 separate measurements of the effects of New England seasonal snow cover on acoustic pulse propagation in the atmosphere have been presented. The measurements show that, when a snow cover is present, the acoustic waveform shape, peak sound-pressure levels, and sound attenuation rates are very different from those measured under summer conditions. An automatic waveform inversion method was successfully implemented and was able to determine unique snow parameters that gave excellent agreement between the measured and calculated acoustic waveforms. The effective flow resistivities determined using this automatic inversion method agree with previous acoustic measurements on snow. The acoustically determined snow depths agreed with the directly measured depths, except for a single case where the depth to a snow layer interface was found. Also, except for a single measurement over newly fallen snow, the pore shape factor ratios determined by the inversion procedure clustered into two groups that may indicate the presence or absence of liquid water within the snowpack. Additional measurements will be made over snow and other winter ground conditions to continue this investigation of environmentally induced variations in acoustic propagation.

In the future, the theoretical approach will be improved in three ways. First, the inversion method will be expanded to include layers within the snow, rather than treating it as a single layer. This modification may allow the snow cover stratigraphy to be determined acoustically. However, the

unique solution found for a single layer may disappear when multiple layers are included. The second improvement will be to implement a jumping approach[65] to select the next parameters in the inversion search. Because the error surface is smooth, this approach should significantly speed up the calculations needed to match the waveforms. Finally, incorporating rigid porous ground impedance models that explicitly include the pore-size distribution as a parameter may offer an improved understanding of the results and additional knowledge of the properties of the snow cover.

Since the effective flow resistivity is proportional to the dynamic viscosity of air divided by the snow permeability, this acoustic waveform inversion method may lead to a useful method of determining snow permeability, a parameter that is currently difficult to measure but of great importance in snow science. Acoustic measurements also have the advantage of determining a spatially averaged permeability value at a scale selectable by the propagation path. This capability is an improvement over current laboratory and field measurements, which are limited to point samples and small sample sizes. Scales could be selected on the basis of the geophysical parameter of interest, and measurements along different directions could be used to investigate, for example, the influence of sastrugi (large surface wind crusts) on snow or firn ventilation for ice core studies. Direct comparison of acoustically determined and conventionally measured[66,67] snow permeabilities are planned in the near future.

ACKNOWLEDGMENTS

These experiments could not have been conducted without the assistance of many of my co-workers. Nancy Greeley provided all the meteorological data, did much of the snow characterization, and assisted with the experiments. Steve Decato was the primary shooter and provided much additional support. Dave Gaskin helped to arrange for the use of the test site and Jim Cragin provided access to a heated shelter for the equipment and personnel. Their assistance is greatly appreciated. Thanks are also due to LT Karen Faran, Gus Greeley, SSG Tommie Hall, Mark Moran, and Frank Perron for their help. Technical reviews were provided by Gilles Daigle and Mark Moran. The author especially appreciated comments from the Associate Editor, Lou Sutherland, and two anonymous reviewers, which greatly improved the clarity of the paper. This work is supported by the Directorate of Research and Development, U.S. Army Corps of Engineers.

[1] K. Attenborough, ''Ground parameter information for propagation modeling,'' J. Acoust. Soc. Am. **92**, 418–427 (1992).
[2] T. F. W. Embleton, J. E. Piercy, and N. Olson, ''Outdoor sound propagation over ground of finite impedance,'' J. Acoust. Soc. Am. **59**, 267–277 (1976).
[3] T. F. W. Embleton, J. E. Piercy, and G. A. Daigle, ''Effective flow resistivity of ground surfaces determined by acoustical measurements,'' J. Acoust. Soc. Am. **74**, 1239–1244 (1983).
[4] D. G. Albert and J. A. Orcutt, ''Observations of low frequency acoustic-to-seismic coupling in the summer and winter,'' J. Acoust. Soc. Am. **86**, 352–359 (1989).
[5] R. A. Sommerfeld, ''A review of snow acoustics,'' Rev. Geophys. Space Phys. **20**, 62–66 (1982).
[6] G. Seligman, ''Sound absorption of snow,'' Nature (London) **143**, 1071 (1939).
[7] S. W. Colliander, ''Russian ski patrols in action,'' Befael **37**(1), 22–25 (1954).
[8] G. W. C. Kaye and E. J. Evans, ''Sound absorption of snow,'' Nature (London) **143**, 80 (1939).
[9] R. B. Watson, ''On the propagation of sound over snow,'' J. Acoust. Soc. Am. **20**, 846–848 (1948).
[10] T. Ishida and S. Onodera, ''Sound absorption by a snow layer,'' Low Temp. Sci., Ser. A **12**, 17–24 (1954).
[11] T. Ishida, ''Acoustic impedance of a snow layer,'' Low Temp. Sci., Ser. A **15**, 81–91 (1956).
[12] T. Ishida, ''Acoustic impedance of a snow layer II,'' Low Temp. Sci., Ser. A **16**, 241–248 (1957).
[13] T. Ishida and H. Shimizu, ''Resistance to air flow through snow layers (Part 1),'' SIPRE Translation 60 [Translation of Low Temp. Sci., Ser. A **14**, 32–42 (1955)] (1958).
[14] T. Ishida, ''Acoustic properties of snow,'' Low Temp. Sci., Ser. A **20**, 23–63 (1965).
[15] H. Oura, ''Reflection of sound at snow surface,'' Seppyo **12**, 273–275 (1950).
[16] H. Oura, ''Sound velocity in snow cover,'' Low Temp. Sci. Ser. A **9**, 171–178 (1953).
[17] H. Oura, ''Reflection of sound at snow surface and mechanism of sound propagation in snow,'' Low Temp. Sci. Ser. A **9**, 179–186 (1953).
[18] H. Oura, ''A study on the optical and the acoustical properties of the snow cover,'' General Assembly of Rome, 1954, IASH Publication No. 4, pp. 71–81 (1954).
[19] S. M. Lee and J. C. Rodgers, ''Characterization of snow by acoustic sounding: A feasibility study,'' J. Sound Vib. **99**, 247–266 (1985).
[20] J. G. Tillotson, ''Attenuation of sound over snow-covered fields,'' J. Acoust. Soc. Am. **39**, 171–173 (1965).
[21] H. Gubler, ''Artificial release of avalanches by explosives,'' J. Glaciol. **19**, 419–429 (1977).
[22] J. B. Johnson, ''On the application of Biot's theory to acoustic wave propagation in snow,'' Cold Regions Sci. Technol. **6**, 49–60 (1982).
[23] M. A. Biot, ''Theory of propagation of elastic waves in a fluid-saturated porous solid. I. Low-frequency range,'' J. Acoust. Soc. Am. **28**, 168–178 (1956).
[24] M. A. Biot, ''Theory of propagation of elastic waves in a fluid-saturated porous solid. II. Higher frequency range,'' J. Acoust. Soc. Am. **28**, 179–191 (1956).
[25] M. A. Biot, ''Mechanics of deformation and acoustic propagation in porous media,'' J. Appl. Phys. **33**, 1482–1498 (1962).
[26] K. Attenborough, ''Review of ground effects on outdoor sound propagation from continuous broadband sources,'' Appl. Acoust. **24**, 289–319 (1988).
[27] M. E. Delaney and E. N. Bazley, ''Acoustical properties of fibrous absorbent materials,'' Appl. Acoust. **3**, 105–116 (1970).
[28] K. Attenborough, ''Acoustical impedance models for outdoor ground surfaces,'' J. Sound Vib. **99**, 521–544 (1985).
[29] J. Nicolas, J.-L. Berry, and G. A. Daigle, ''Propagation of sound above a finite layer of snow,'' J. Acoust. Soc. Am. **77**, 67–73 (1985).
[30] H. M. Moore, K. Attenborough, J. Rogers, and S. Lee, ''*In situ* acoustical investigations of deep snow,'' Appl. Acoust. **33**, 281–301 (1991).
[31] D. G. Albert and J. A. Orcutt, ''Acoustic pulse propagation above grassland and snow: Comparison of theoretical and experimental waveforms,'' J. Acoust. Soc. Am. **87**, 93–100 (1990).
[32] O. Buser, ''A rigid frame model of porous media for the acoustic impedance of snow,'' J. Sound Vib. **111**, 71–92 (1986).
[33] K. Attenborough and O. Buser, ''On the application of rigid-porous models to impedance data for snow,'' J. Sound Vib. **124**, 315–327 (1988).
[34] S. C. Colbeck, ''An overview of seasonal snow metamorphism,'' Rev. Geophys. Space Phys. **20**(1), 45–61 (1982).
[35] S. Colbeck, E. Akitaya, R. Armstrong, H. Gubler, J. Lafeuille, K. Lied, D. McClung, and E. Morris, ''International Classification for Seasonal Snow on the Ground,'' International Comm. Snow and Ice (IAHS), World Data Center A for Glaciology, University of Colorado, Boulder (1990).
[36] D. G. Albert, ''Observations of acoustic surface waves propagating above a snow cover,'' *Proceedings of the Fifth International Conference on Long Range Sound Propagation* (The Open University, Milton Keynes, England, 1992), pp. 10–16.
[37] H. A. J. M. van Hoof and K. W. F. M. Doorman, ''Coupling of airborne sound in a sandy soil,'' TNO/LEOK Rep. No. TR 1983-09, Netherlands

Organization for Applied Scientific Research, Laboratory for Electronic Developments for the Armed Forces, Oegstgeest, NL (1983).
[38] C. Madshus and A. M. Kanyia, ''Ground response to propagating airblast,'' *Inter-Noise 96* (Institute of Acoustics, Liverpool, UK, 1996), pp. 1433–1438.
[39] H. E. Bass, L. N. Bolen, D. Cress, J. Lundien, and M. Flohr, ''Coupling of airborne sound into the earth: Frequency dependence,'' J. Acoust. Soc. Am. **67**, 1502–1506 (1980).
[40] J. M. Sabatier, H. E. Bass, and L. N. Bolen, ''Acoustically induced seismic waves,'' J. Acoust. Soc. Am. **80**, 646–649 (1986).
[41] A. J. Cramond and C. G. Don, ''Reflection of impulses as a method of determining acoustic impedance,'' J. Acoust. Soc. Am. **75**, 382–389 (1984).
[42] C. G. Don and A. J. Cramond, ''Soil impedance measurements by an acoustic pulse technique,'' J. Acoust. Soc. Am. **77**, 1601–1609 (1985).
[43] R. Raspet, H. E. Bass, and J. Ezell, ''Effect of finite ground impedance on the propagation of acoustic pulses,'' J. Acoust. Soc. Am. **74**, 267–274 (1983).
[44] R. Raspet, J. Ezell, and H. E. Bass, Additional comments on and erratum for ''Effect of finite ground impedance on the propagation of acoustic pulses'' [J. Acoust. Soc. Amer. **74**, 267–274 (1983)], J. Acoust. Soc. Am. **77**, 1955–1958 (1985).
[45] A. J. Cramond and C. G. Don, ''Effects of moisture content on soil impedance,'' J. Acoust. Soc. Am. **82**, 293–301 (1987).
[46] C. G. Don and A. J. Cramond, ''Impulse propagation in a neutral atmosphere,'' J. Acoust. Soc. Am. **81**, 1341–1349 (1987).
[47] K. Attenborough, S. I. Hayek, and J. M. Lawther, ''Propagation of sound above a porous half-space,'' J. Acoust. Soc. Am. **68**, 1493–1501 (1980).
[48] K. U. Ingard, ''On the reflection of a spherical wave from an infinite plane,'' J. Acoust. Soc. Am. **23**, 329–335 (1951).
[49] I. Rudnick, ''Propagation of an acoustic wave along a boundary,'' J. Acoust. Soc. Am. **19**, 348–356 (1947).
[50] L. M. Brekhovskikh, *Waves in Layered Media*, 2nd ed. (Academic, New York, 1980).
[51] J. F. Allard, *Propagation of Sound in Porous Media* (Elsevier, London, 1993), p. 284.
[52] S. C. Constable, R. L. Parker, and C. G. Constable, ''Occam's inversion: A practical algorithm for generating smooth models from electromagnetic sounding data,'' Geophysics **52**, 289–300 (1987).
[53] W. H. Press, B. P. Flannery, S. A. Teukolsky, and W. T. Vetterling, *Numerical Recipes: The Art of Scientific Computing* (Cambridge University Press, New York, 1986).
[54] R. Jordan, ''Effects of capillary discontinuities on water flow and water retention in layered snow covers,'' International Symposium on Snow and Related Manifestations, Manali, India (1994).
[55] D. Hillel and R. S. Baker, ''A descriptive theory of fingering during infiltration into layered soils,'' Soil Sci. **146**, 51–56 (1988).
[56] H. M. Hess, K. Attenborough, and N. W. Heap, ''Ground characterization by short-range propagation measurements,'' J. Acoust. Soc. Am. **87**, 1975–1986 (1990).
[57] J. M. Sabatier, H. Hess, W. P. Arnott, K. Attenborough, M. J. M. Roemkens, and E. H. Grissinger, ''*In situ* measurements of soil physical properties by acoustical techniques,'' Soil Sci. Soc. Am. J. **54**, 658–672 (1990).
[58] Care is needed in comparing these values with other work, since in many cases a different definition of effective flow resistivity is used. For example, Hess *et al.* (Ref. 56) use $\sigma_{pe}=\frac{1}{4}s_f^2\Omega\sigma$. Reducing the values reported here according to the above definition gives agreement with Hess *et al.*'s low reported values of 1 to 3 kN s m^{-4}.
[59] Y. Champoux and M. R. Stinson, ''On acoustical models for sound propagation in rigid frame porous materials and the influence of shape factors,'' J. Acoust. Soc. Am. **92**, 1120–1131 (1992).
[60] M. R. Stinson and Y. Champoux, ''Propagation of sound and the assignment of shape factors in model porous materials having simple pore geometries,'' J. Acoust. Soc. Am. **91**, 685–695 (1992).
[61] K. Attenborough, ''Models for the acoustical properties of air-saturated granular media,'' Acta Acust. (China) **1**, 213–226 (1993).
[62] D. K. Wilson, ''Relaxation-matched modeling of propagation through porous media, including fractal pore structure,'' J. Acoust. Soc. Am. **94**, 1136–1145 (1993).
[63] T. Yamamoto and A. Turgut, ''Acoustic wave propagation through porous media with arbitrary pore size distribution,'' J. Acoust. Soc. Am. **83**, 1744–1751 (1988).
[64] D. G. Albert, ''Environmental effects on acoustic wave propagation at Ft. Greely, Alaska,'' *1998 Meeting of the IRIS Specialty Group on Acoustic and Seismic Sensing* (Johns Hopkins University, Laurel, MD, 1999), pp. 273–280.
[65] P. R. Shaw and J. A. Orcutt, ''Waveform inversion of seismic refraction data and applications to young Pacific crust,'' Geophys. J. R. Astron. Soc. **82**, 375–414 (1985).
[66] E. F. Chacho, Jr. and J. B. Johnson, ''Air permeability of snow,'' EOS Trans. Am. Geophys. Union **68**, 1271 (abstract) (1987).
[67] J. P. Hardy and D. G. Albert, ''The permeability of temperate snow: Preliminary links to microstructure,'' Proceedings of the 50th Eastern Snow Conference, Quebec, Canada (1993), pp. 149–156.